

Structure and electronic properties of new model dinitride systems: A density-functional study of CN_2 , SiN_2 , and GeN_2

R. Wehrich^{1,2}, V. Eyert^{1,3*}, S. F. Matar¹

¹*Institut de Chimie de la Matière Condensée de Bordeaux, I.C.M.C.B-CNRS, 33608 Pessac Cedex, France,*

²*Anorganische Chemie, Universität Regensburg, 93040 Regensburg, Germany,*

³*Institut für Physik, Universität Augsburg, 86135 Augsburg, Germany*

Abstract

The dinitrides CN_2 , SiN_2 , and GeN_2 in assumed pyrite-type structures are studied by means of density functional theory using both ultrasoft pseudopotentials and the augmented spherical wave (ASW) method. The former two materials constitute the large-x limit of the broader class of CN_x and SiN_x compounds, which are well known for their interesting mechanical and electronic properties. For CN_2 a large bulk modulus B_0 of 405 GPa was determined. While SiN_2 is found to be a wide band gap compound, the calculated gaps of CN_2 and GeN_2 are considerably smaller. The trends in structural and electronic properties as e.g. bond lengths, band gaps and covalency are well understood in terms of the interplay of different types of bonding.

Key words: density functional theory, ultra hard materials, pyrite-type structure

PACS: 62.25.+g, 71.15.Mb, 71.20.Nr

1 Introduction

In recent years nitrogen has turned out to play a key role in today's most exciting technological applications of materials science. Important examples are the development of III-V nitrides (AlN, GaN, InN) for light emitting diodes (LED) and lasers [1,2], the investigation of Si_3N_4 and SiO_xN_y as promising candidates for ultrathin high dielectric materials substituting SiO_2 in the race

* Corresponding author. fax: +49 821 598 3262

Email address: eyert@physik.uni-augsburg.de (V. Eyert^{1,3}).

for ever shrinking field effect transistor (FET) gate lengths [3], and, finally, new ultra hard materials with the proposal of a model carbon nitride C_3N_4 as the hardest known material [4]. However, all attempts to grow thin layers of nitrogen rich stoichiometries failed because of the easy release of nitrogen due to the high stability of molecular N_2 [5]. This major drawback led to propose nitrogen poor stoichiometries such as $C_{11}N_4$ [6]. Nevertheless, the process of N_2 release from CN_x has not yet been investigated in detail and only recently a preliminary approach based on a model structure CN_2 was presented [7]. However, our knowledge about this class of nitride systems is far from exhaustive. To some extent this is due to the fact that the search for compounds with new materials properties is not straightforward and can be experimentally very demanding. In this situation, state-of-the-art computer simulations built on the principles of quantum mechanics as embodied in density functional theory (DFT) are very helpful. In particular, they even allow to investigate compounds, which are not yet synthesized.

Aiming at a deeper understanding of ultra hard nitrides we report in the present work on investigations of the lightest IV-V compounds CN_2 , SiN_2 and GeN_2 as crystallizing in an assumed cubic pyrite structure [7]. This choice of hypothetical structure is guided by the observation that it allows to build up C-N bonds in a three-dimensional network while still satisfying the strong N-N bonding. At the same time, the simplicity of the pyrite structure offers the advantage that the different types of bondings can be easily addressed. Finally, this structure is also adopted by other isoelectronic AX_2 compounds, as e.g. SiP_2 [8,9]. Further experimental evidence comes from N- or C-doped SiP_2 and related compounds. In the pyrite structure, the N-N entities occupy octahedral holes formed by the C, Si and Ge fcc sublattices. The latter are well known from the cubic structures of diamond, SiC, SiGe, and TiC. As estimates for amorphous SiN_x [10] and SiN_2 clusters [11] show, CN_2 and SiN_2 represent the large-x limit of those ultra hard and wide electronic band gap CN_x and SiN_x materials, which contain N-N-bonds.

From a chemical point of view, the transition from SiP_2 to SiN_2 , CN_2 , and GeN_2 involves several fundamental issues. These are the behaviour of the light group IV compounds C, Si and Ge in octahedral environments as well as that of nitrogen in the center of tetrahedra formed by one N and three C (Si/Ge) neighbours. The resulting description on the related bonding schemes should be found in between Paulings covalent bonding [12] and ionic concepts like $A^{4+}[N_2]^{4-}$ with the anions isoelectronic to $[S_2]^{2-}$ in pyrite FeS_2 . While $[N_2]^{2-}$ was proposed to appear in diacnides [13], covalent N-N-bonds have been proposed for clustered III-V semiconductor nitrides [14].

In this work we concentrate, using DFT-based methods, on finding the optimal crystal structure parameters of pyrite CN_2 , SiN_2 and GeN_2 . In addition, we aim at relating the crystal structure stability to the electronic properties as well as to the chemical bonding.

2 Computational methods

The electronic structure calculations were performed within the framework of density functional theory and the local density approximation using two complementary approaches. First, full geometry relaxations including optimization of the cell volume and the atomic positions were performed with the help of an ultrasoft pseudopotential scheme as implemented in the VASP code [15,16,17,18]. Calculations were converged at an energy cutoff of 434.82 eV for the plane-wave basis set. The Brillouin zone integration was performed using 11 to 76 irreducible \mathbf{k} points and the tetrahedron method [19].

In a second step, the electronic properties of all three compounds were determined using the all-electron augmented spherical wave (ASW) method [20,21]. In order to represent the correct shape of the crystal potential in the large voids, additional augmentation spheres were inserted into the open pyrite structure. Optimal augmentation sphere positions as well as radii of all spheres were automatically generated by the sphere geometry optimization (SGO) algorithm [22]. The basis sets comprised s , p , and $3d$ states of the group IV element, N $2s$, $2p$ states as well as states of the additional augmentation spheres. The Brillouin zone integration was done using an increasing number of \mathbf{k} points within the irreducible wedge ranging from 11 to 1135 points, again to ensure convergence of the results with respect to the \mathbf{k} -space grid.

3 Results and Discussion

3.1 Crystal structure optimization

The pyrite structure AX_2 is best described in terms of the rocksalt structure with the A atoms and X_2 occupying the two sublattices such that cubic symmetry with space group $Pa\bar{3}$ is preserved [23]. As a result, the A atoms are found at the center of X_6 octahedra, while three A atoms and one X atom form distorted tetrahedra about the X sites, see Fig. 1. The pyrite structure is fully specified by two parameters, namely, the lattice constant and the positional parameter x of the X atoms.

To start with, we performed a structural optimization for SiP_2 , where the theoretical results could be checked against experimental data [8], see Tab. 1. As expected, the lattice constant is slightly underestimated by the LDA calculations. In contrast, the internal parameter x_P is almost exactly reproduced and so is the fraction $\frac{d_{X-X}}{d_{A-X}}$, with the P-P distance being shorter than the Si-P bond.

On going to the nitride we observe a drastic volume decrease with a calculated lattice constant of ≈ 4.42 Å close to the value of 4.348 Å measured for

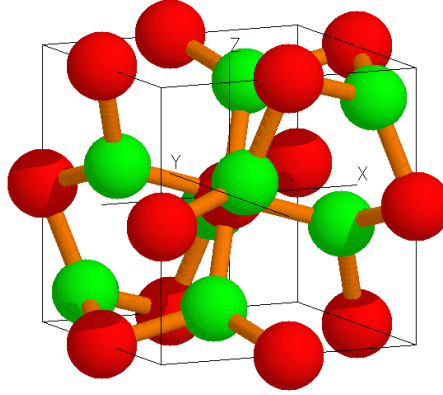


Fig. 1. Pyrite structure. Group IV element atoms are found at the centers of the cube and the edges, respectively.

		E	V	a	x_X	d_{X-X}	d_{A-X}	$\frac{d_{X-X}}{d_{A-X}}$
SiP ₂	exp			5.7060	0.3906	2.162	2.397	0,902
SiP ₂	LDA	-6.213	180.85	5.6551	0.3905	2.145	2.376	0,903
SiN ₂	LDA	-8.806	86.32	4.4195	0.4050	1.454	1.886	0,771
CN ₂	LDA	-7.948	63.13	3.9818	0.4029	1.339	1.695	0,790
GeN ₂	LDA	-7.785	100.37	4.6474	0.4113	1.428	1.998	0,715

Table 1

Crystallographic data of the optimized structures. Lengths in Å and energies in eV/atom. Experimental data taken from Ref. [8].

SiC [24]. In addition, the distance fraction $\frac{d_{X-X}}{d_{A-X}}$ has considerably decreased. While the N-N bond length amounts to 1.454 Å, the Si-N distance of 1.886 Å is very similar to the corresponding value of 1.889 Å observed for Si₃N₄ and is indicative of a single bond. For GeN₂, our calculations yield a bigger cell, albeit, with a still shorter N-N distance of 1.428 Å.

Finally, optimizing the pyrite structure for CN₂, we obtain an even smaller lattice constant of 3.982 Å. Together with the calculated internal parameter of $x_N = 0.403$ this leads to an N-N distance of 1.34 Å. While still being much larger than in molecular N₂ (1.09 Å), this value is considerably smaller than in SiN₂ and GeN₂ strengthening the double bond. At the same time the C-N distance of 1.695 Å is significantly larger than the 1.47 Å measured for the C-N single bonds of C₃N₄ indicating an even lower order. Applying the usual estimates for the hardness of CN_x compounds [25,26] we calculate a bulk modulus of $B_0 = 405$ GPa from a Birch fit [27]. Since this is harder than cubic BN, CN₂ in the pyrite type structure may be regarded as a high-density ultra hard material. Since the energy values given in Tab. 1 are relative to the atomic energies and thus not indicative for the stability of the compounds, we

performed additional supercell calculations for atomic C (Si, Ge) as well as molecular N₂ and obtained a heat of formation of -4 eV/atom.

3.2 Electronic structure

The band structure of CN₂ along selected high symmetry lines within the first Brillouin zone of the simple cubic lattice [23] as well as the partial densities of states (DOS) of all three compounds are shown in Figs. 2 and 3. In these figures

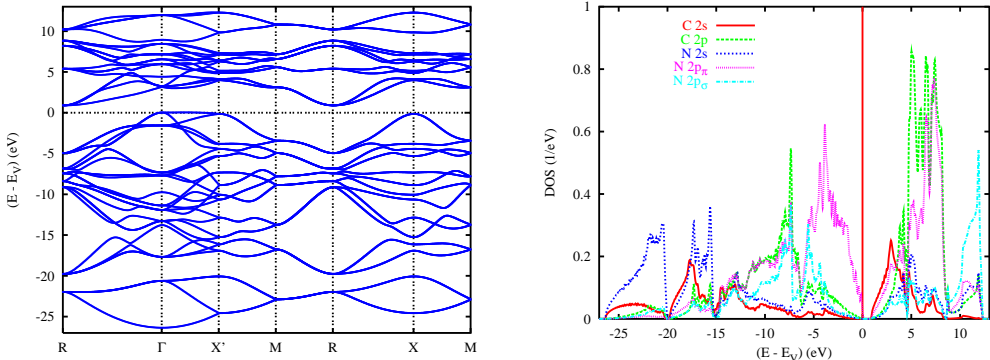


Fig. 2. Electronic structure and partial densities of states (DOS) of CN₂.

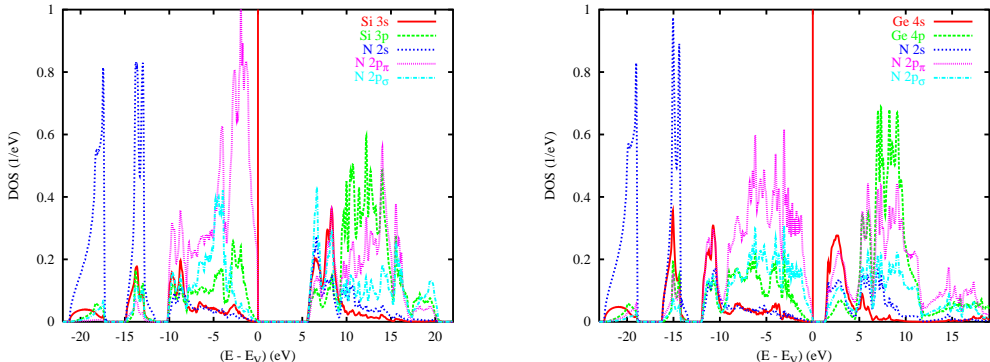


Fig. 3. Partial densities of states (DOS) of SiN₂ and GeN₂.

four groups of bands are identified. The two low-energy groups of bands each comprise four single bands. Bands are most easily counted along the line M-R, where they are fourfold degenerate. According to the partial densities of states these bands trace back mainly to the N 2s states, which form a bonding and antibonding subset of several eV width. Whereas the large splitting between these two groups is due to the short N-N distance the intrinsic band widths of both groups mainly result from the dispersion across the face-centered cubic (fcc) lattice formed by the nitrogen pairs. This is concluded from the level sequence at the Γ point into a lower nondegenerate and an upper threefold

degenerate state. The latter results from folding the fcc bands into the simple cubic Brillouin zone (for the antibonding group of bands the sequence of levels is reversed). Further support comes from the striking similarity of the density of states especially of the bonding bands to that of a band calculated within the tight-binding approximation for an fcc lattice. Band widths are largest for CN_2 , which has the smallest lattice constant.

The electronic structure of the valence and conduction band are influenced by different types of bondings. Both groups comprise 20 bands, which derive from hybridization of all orbitals except for the N $2s$ states. Note that we have used a rotated coordinate system to separate the N $2p$ partial densities of states into contributions from orbitals mediating σ - and π -type bonding within the N_2 pairs. The calculated optical band gaps are 0.9, 5.5, and 1.4 eV for CN_2 , SiN_2 and GeN_2 , respectively.

Common to all three nitrides is the strong bonding between group IV element p states and those of nitrogen, which leads to bonding and antibonding bands in the energy regions [-12:-6] and [5:9] eV for CN_2 , [-10:-4] and [10:15] eV for SiN_2 , and [-9:0] and [5:18] eV for GeN_2 , respectively. Since the nitrogen atoms are coordinated by three group IV atoms this bonding is rather isotropic and, hence, involves both the $2p_\sigma$ and $2p_\pi$ states in the same manner with the ratio of 1:2 of their partial DOS reflecting their respective weight. Except for the carbon compound the unoccupied antibonding bands are dominated by the group IV element p states, whereas the N $2p$ orbitals show a larger contribution to the bonding bands.

Differences between the three compounds, which cause, in particular, the spread in calculated optical band gaps, can be traced back mainly to the different influence of two additional types of bonding. These are, respectively, the bonding between the group IV element s and the N $2sp$ states as well as the strong σ - and π -type overlap within the nitrogen pairs. The former leads to considerable contributions of the C/Si/Ge s states to the second group of bands as well as to the lower edges of the valence and conduction bands. Across the series, s - p hybridization of the group IV element decreases and, on going from C to Ge, the bonding and antibonding bands involving the s states are lowered in energy relative to the bands derived from the group IV element p states. This effect is already visible for SiN_2 and becomes most obvious for GeN_2 , where it leads to the substantial decrease of the optical band gap.

To the contrary, the σ - and π -type overlap within the N_2 pairs causes splitting of the $2p_\sigma$ and $2p_\pi$ states into bonding and antibonding bands. In the partial DOS, those N $2p$ states, which are subject to overlap within the pairs, can be easily identified by the smaller C/Si/Ge contributions in the respective energy range. However, due to the large N-N distance in both SiN_2 and GeN_2 , this bonding/antibonding splitting is rather weak in these two nitrides. This is contrasted by the situation in CN_2 , where the close coupling of the nitrogen atoms leads to strong splitting into bonding and antibonding bands showing up in the energy intervals from [-6:0] and [8:12] eV, respectively. To conclude, the N $2p$ states are subject to two different types of bonding, namely, that inside the

pairs and that with the group IV element sp states. The bonding and antibonding states resulting from both types of chemical bonds end up in different energy regions. In particular, for CN_2 the bonding bands resulting from N-N $2p$ overlap are higher in energy than the bands growing out of C/Si/Ge sp -N $2p$ overlap. As a consequence, the optical band gap is considerably reduced as compared to SiN_2 .

4 Conclusions

First principles calculations for the dinitrides CN_2 , SiN_2 and GeN_2 in assumed pyrite-type structures result in stable crystals. A bulk modulus of $B_0 = 405$ eV is calculated for CN_2 , which thus can be regarded as an ultra hard material. The electronic structures of all three nitrides are governed by three different types of bonding. Overlap of the C/Si/Ge s and p orbitals with the N $2p$ states lead to the formation of bonding and antibonding bands, which give rise to the valence and conduction groups of bands, respectively. In both groups, the C/Si/Ge s derived states are found at the lower band edge. Lowering of the s states relative to the p states due to decreasing s - p hybridization across the series C-Si-Ge results in a depression of the optical band gap of GeN_2 as compared to that of SiN_2 . Close coupling within the N_2 pairs especially in CN_2 gives rise to a third type of bonding, namely σ - and π -type overlap of the N $2p$ states. The resulting bonding and antibonding bands are found at the upper edges of the valence and conduction bands of CN_2 and again lead to a strong decrease of the optical band gap as compared to SiN_2 .

Acknowledgements

We are grateful to Profs. K.-J. Range and J. Etourneau for a lot of fruitful discussions, continuous interest, and support of this work. R. W. and V. E. gratefully acknowledge the kind hospitality of the ICMCB and the University Bordeaux 1. R. W. acknowledges financial support by the Training and Mobility Network "New carbon based ultra hard Materials", 1997-2002 "FMRX-CT97-0103 (DG 12-MSPS)". This work was supported by the Deutsche Forschungsgemeinschaft through SFB 484, Augsburg. Calculations were done on the Regatta IBM P690 of the M3PEC intensive numerical computations facility of the University Bordeaux 1.

References

- [1] S. Nakamura, J. Appl. Phys. 74 (1993) 3911.
- [2] K. Okada, Y. Yamada, T. Taguchi, F. Sasaki, S. Kobayashi, T. Tani, S. Nakamura, and G. Shinomiya, Jap. J. Appl. Phys. 35 (1996) L787.
- [3] N. Konofaos and E. K. Evangelou, Semicond. Sci. Technol. 18 (2003) 56.
- [4] D. M. Teter and R. J. Hemley, Science 271 (1996) 53.
- [5] N. Hellgren, PhD thesis, Linköping University 1999.
- [6] A. Snis and S. F. Matar, Phys. Rev. B 60 (1999) 10885.
- [7] R. Weihrich, S. F. Matar, V. Eyert, and E. Betranhandy, Solid State Sciences xx (2003) xxx.
- [8] T. K. Chattopadhyay and H. G. v. Schnering, Z. Krist. 167 (1984) 1.
- [9] N. E. Brese and H. G. v. Schnering, Z. Anorg. Allg. Chem. 620 (1994) 393.
- [10] L. Martn-Moreno, E. Martinez, J. A. Vergs, and F. Yndurain, Phys. Rev. B 35 (1987) 9683.
- [11] Y.-C. Bae, H. Osanai, K. Ohno, M. Sluiter, and Y. Kawazoe, Mat. Trans. 43 (2002) 482.
- [12] L. Pauling, *The Nature of the Chemical Bond*, Cornell University Press, Cornell 1960.
- [13] G. Auffermann, Y. Prots, and R. Kniep, Angew. Chem. Int. Ed. Engl. 40 (2001) 547.
- [14] A. Costales, M. Blanco, A. M. Pendas, M. Angerl, A. K. Kandalam, and R. Pandey, J. Am. Chem. Soc. 124 (1992) 4116.
- [15] G. Kresse and J. Hafner, Phys. Rev. B 47 (1993) 558.
- [16] G. Kresse and J. Hafner, Phys. Rev. B 49 (1994) 14251.
- [17] G. Kresse and J. Furthmüller, Comput. Mat. Sci. 6 (1996) 15.
- [18] G. Kresse and J. Furthmüller, Phys. Rev. B 54 (1996) 11169.
- [19] P. E. Blöchl, O. Jepsen, and O. K. Anderson, Phys. Rev. B 49 (1994) 16223.
- [20] A. R. Williams, J. Kübler, and C. D. Gelatt jr., Phys. Rev. B 19 (1979) 6094.
- [21] V. Eyert, Int. J. Quant. Chem. 77 (2000) 1007.
- [22] V. Eyert and K.-H. Höck, Phys. Rev. B 57 (1998) 12727.
- [23] V. Eyert, K.-H. Höck, S. Fiechter, and H. Tributsch, Phys. Rev. B 57 (1998) 6350.

- [24] P. Villars and L. D. Calvert, *Pearson's Handbook of Crystallographic Data for Intermetallic Phases*, American Society for Metals, Materials Park 1991.
- [25] M. Mattesini, S. F. Matar, A. Snis, J. Etourneau, and A. Mavromaras, *J. Mater. Chem.* 10 (2000) 709.
- [26] M. Mattesini and S. F. Matar, *Phys. Rev. B* 65 (2002) 075110.
- [27] F. Birch, *J. Geophys. Res.* 83 (1978) 1257.